Abstract

The intensive worldwide use of rectangular hollow sections (RHS) structural elements, mainly due to its associated aesthetical and structural advantages, led designers to be focused on the technologic and design aspects of these structures. As a consequence, the accuracy of their design methods is of major importance both under the economical and safety points of view.

Recent studies in the field of connections in RHS structures seem to point out for further research needs, especially for some particular geometries. This is particularly significant when the failure mode changes and the prediction of the failure load may be unsafe or uneconomical.

In this paper a numerical based parametric study is presented, for the analysis of a "T" joint configuration where both the chord and brace are made of RHS sections. Starting from test results available in the literature and from previous numerical models and studies, a model has been derived, taking into account the weld geometry, material and geometric nonlinearities, and was validated by comparison to published experiments.

The main variable of the study was the brace width to chord width ratio. The choice of this parameter was based on recent studies results that depicted some Eurocode 3 rules discrepancies for particular values of this parameter, mainly due to the shear and bending failure mode interaction.

The numerical results were compared to the analytical results from the Eurocode 3 and to the classic deformation limits proposed in the literature. This is followed by a critical comparison of these results focusing on the most critical aspects of the available analytical formulation and their practical consequences.

Keywords: Steel structures, welded joints, finite element analysis, plastic analysis, non-linear analysis.

1 Introduction

Structural hollow sections (Figure 1) are widely used by designers, since they have many aesthetical and structural advantages [15], [18]. On the other hand, they lead quite frequently to more expensive and difficult connections, since there is no access to the interior of the connected parts. This problem is solved by special blind bolted connections, or more frequently, by the extensive use of welded connections. Besides the matter of fabrication costs, connections have to be properly taken into account in the design, since their behaviour frequently governs the overall structural response. This paper deals with the structural behaviour of RHS "T" joints (Figure 2) in trusses under static loading. The effects of shear, punching shear and bending are taken into account to predict the failure of the joint.

Figure 1 – Examples of tubular structures

Traditionally, design rules for hollow sections joints are based either on plastic analysis either on deformation limits criteria.

The use of plastic analysis to define the joint ultimate limit sate is based on a plastic mechanism corresponding to the assumed yield line pattern. As examples, the studies of Cao *et al* [2], Packer [17], Packer *et al* [15] and Kosteski *et al* [7] may be referred. Each plastic mechanism is associated to an ultimate load, more accurate for more adequate mechanisms. These authors adopted for the yield lines, straight, circular, or a combination of both patterns. Packer et al [16] have assumed these three patterns, concluding that the best approximation (if compared to experimental results) was the straight lines mechanism, with an optimising parameter.

However, some of these authors found that for large values of the parameter β (β is the brace width to chord width – see Figure 2), these mechanisms could give a very poor and unsafe prediction of the ultimate load. In fact, the solutions from these bending mechanisms tend to infinity when the parameter β tends to 1 (Figure 3). Packer *et al* [15] found that when $\beta \geq 0{,}95$ the theoretical bending load could be of only 12% of the corresponding experimental load. These authors have then proposed pure shear mechanisms, and concluded that their application to these cases overestimate the experimental load as well, with the theoretical load of only 30% of the corresponding experimental load. Similar conclusions were pointed out by the authors in [13].

Davies and Packer [3] have proposed plastic mechanisms taking into account bending and punching shear, and found that the corresponding results are a considerable improvement of accuracy, since they overestimate the experimental load of about 20%.

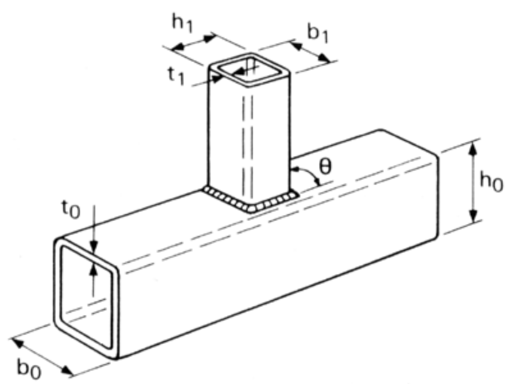

$$\beta = \frac{b_1}{b_0} \qquad (1)$$

$$\mu_1 = \frac{b_1}{t_1} \qquad (2)$$

$$\mu_0 = \frac{b_0}{t_0} \qquad (3)$$

$$\gamma = \frac{b_0}{2t_0} \qquad (4)$$

Figure 2: Geometry and governing parameters.

Gomes [5], in the context of minor axis joints, developed plastic mechanisms with yield log-spiral fans that considerably reduce the plastic load for bending, as shown in Figure 3. This author developed as well mechanisms taking into account bending and punching shear simultaneously, all directly applicable to RHS joints but not, until the present, adopted in any code provisions.

Deformation limits criteria usually associate the ultimate limit state of the chord face to a maximum out of plane deformation of this component. Korol and Mirza [6] proposed that the ultimate limit state should be associated to a chord face displacement of 1.2 times its thickness, as this value corresponded to about 25 times the chord face elastic deformation. Lu *et al* [12] proposed that the joint ultimate limit state should be associated to an out of plane deformation equal to 3% of the face width, corresponding to the maximum load reached in their experimental study. This 3% limit was proposed as well by Zhao [20], and is actually adopted by the International Institute of Welding to define the ultimate limit state.

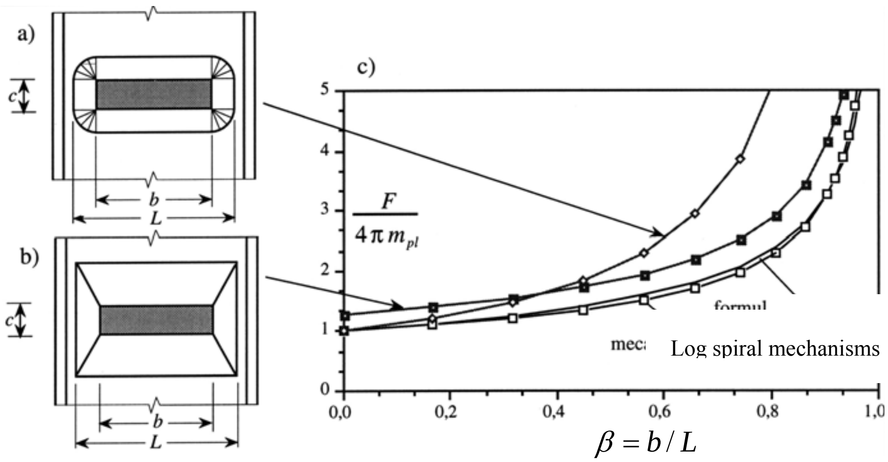

Figure 3: Log spiral mechanisms and other patterns mechanisms.

Kosteski *et al* [7] have compared results from the plastic analysis to the above referred deformation limit (3%), and concluded that if punching shear is not the ruling mechanism, results are within a 20 % approximation range.

The justification for a deformation limit criterion instead of the use of plastic analysis for the prediction of the ultimate limit state is that, for slender chord faces, the joint stiffness does not vanish after complete yielding, but may assume quite large values due to membrane effects. This phenomenon is clearly shown in the curves obtained from the material and geometrical nonlinear analysis in the context of the present study. It is evident that, if the maximum load is obtained from experimental curves, the absence of a "knee" in the curve could make difficult to identify this ultimate limit state point. Besides, comparison of experimental and plastic analysis results need, in these cases, to be based on a deformation criterion as well.

The full exploitation of this additional membrane resistance is not compatible with the allowed displacements within the joint. Besides, if the chord is subjected to cyclic loading, or the chord is subjected to compressive axial loading, membrane over-strength will not be significant anymore [2], [14]. As a consequence, the most effective and correct way to define these joints ultimate limit state, besides adequate numerical or experimental testing, is the analytical way using plastic analysis, incorporating punching shear and instability phenomena.

2 Eurocode 3 Provisions

For connections between RHS joints, such as the represented in Figure 2, the methodology proposed by the Eurocode 3 part 1-8 (EN 1993-1-8) [4] is based on the assumption that these joints are pinned and therefore the relevant characteristic (besides to the deformation capacity) is the resistance of the chord and braces, all subjected primarily to axial forces. Eurocode 3 provisions for the evaluation of this design joint resistance assume the following failure modes:

- plastic failure of the chord face Figure 4(a);
- chord side wall failure by yielding, crushing or instability under the compression brace member Figure 4(b);
- chord yielding (plastic failure of the chord cross section);
- chord shear failure Figure 4(c);
- punching shear failure of a hollow section chord wall Figure 4(d);
- brace failure with reduced effective width Figure 4(e);
- local buckling failure of a brace member, or of an hollow section chord member at the joint location Figure 4(f).

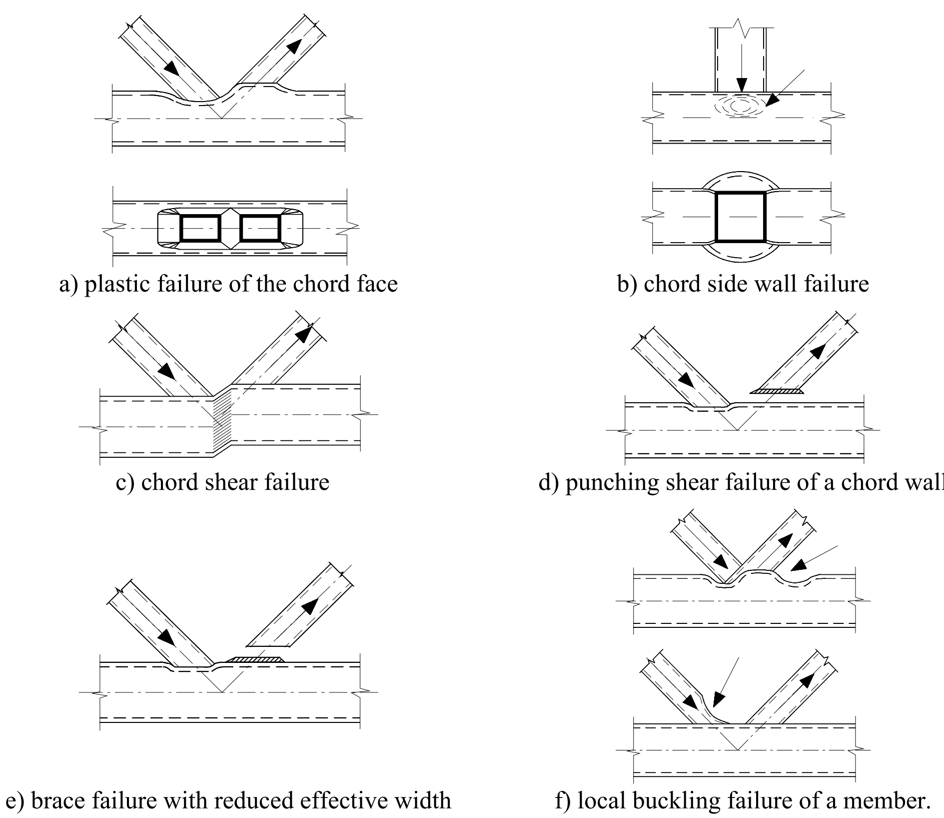

Figure 4: Eurocode3 failure modes [4].

For the "T" joint, the Eurocode provisions consider the failure of the RHS joint by mechanisms a), b), d), e) or f), and assume a range of validity of $\beta \geq 0.25$, $\mu_1 \leq 35$ and $\mu_0 \leq 35$.

For the first structure considered in this work, the chord is 350×15 RHS section and the brace 200×16 RHS section. Therefore, the parameters of Figure 2 take the values of β = 0.57, μ_0 = 23.3, μ_1 = 12.5 and γ_0 = 11.67. The value of β = 0.57 is not critical. However, for values greater than 0.85, since it may be easily observed from Figure 3, that a small variation of β in this zone corresponds to a very substantial variation of the plastic load from a bending mechanism. In addition, the problem in this particular structure is that the value of β is very close to the border between failure modes a) for $\beta \leq 0.85$ and d) $\beta \geq 0.85$.

Equation (5) defines according to Eurocode [4] the plastic load for the chord face, in the case of the "T" joint concerned in this paper, and for the geometric parameters in Figure 2. $N_{1,Rd}$ is the brace axial load leading to yielding or punching of the chord face. To compute this value, equation (5) from the Eurocode [4] should be used if $\beta \leq 0{,}85$:

$$N_{1,Rd} = \frac{k_n f_{y0} t_0^2}{(1-\beta) sen\theta_1}\left(\frac{2\beta}{sen\theta_1} + 4\sqrt{1-\beta}\right) \tag{5}$$

where k_n is 1,0 for tensioned members, f_{y0} is the chord yield stress, t_0 the chord thickness, β is a geometrical parameter defined in Figure 2 and θ_1 the angle between the chord and the brace.

For values of β larger than 0,85 Packer *et al.* [15] and the Eurocode 3 [4] propose to compute the strength for $\beta = 1{,}00$ and for $\beta = 0{,}85$ and then use linear interpolation for the actual value of β. For $\beta = 1{,}00$ the failure due to chord side wall buckling is given by equation (6), and failure involving punching shear by equation (7). However, for this case, the value of β is limited up to $1 - 1/\gamma$, where γ is given in equation (4).

$$N_{1,Rd} = \frac{f_{y0} . t_0}{sen\theta_1}\left[\frac{2h_1}{sen\theta_1} + 10t_0\right] \tag{6}$$

$$N_{1,Rd} = \frac{f_{y0} . t_0}{\sqrt{3} sen\theta_1}\left[\frac{2h_1}{sen\theta_1} + 2b_{e,p}\right] \tag{7}$$

where $b_{e,p}$ is the effective width for punching shear evaluated by $b_{e,p} = 10b_1/(b_0/t_0)$.

4 Numerical Model

4.1 General

A finite element model for the studied geometries was developed using four-nodes thick shell elements, therefore considering bending, shear and membrane deformations. The mesh was more refined near the weld, where the stress concentration is likely to happen, and the more regular as possible, with well proportioned elements to avoid numerical problems.

The material and geometrical properties used in the analysis are presented in Table 1, and are the same used by Lie *et al.* [9], [10] in order to calibrate the mechanical model with the experimental results from these authors. It is important to emphasize that the experimental tests performed by Lie *et al.* [9], [10] considered cracked welds. However, in this reference, a numerical result based on the model without cracks in the weld was presented as well. These results were used to calibrate the finite element model used in this paper and that will be presented in next sections.

Table 1 – Mechanical properties after Lie *et al.* [9].

Specimen	b_0 (mm)	h_0 (mm)	t_0 (mm)	b_1 (mm)	h_1 (mm)	t_1 (mm)	t_w (mm)	f_y (MPa)	f_u (MPa)	f_w (MPa)
T1	350	350	15	200	200	16	12	380.3	529.0	600
T2	350	350	15	200	200	12	12	380.3	529.0	600

Figure 5 shows the finite element model for the “T” joint, composed of 9482 nodes and 9284 elements performed in the Ansys 10.0 package software [1].

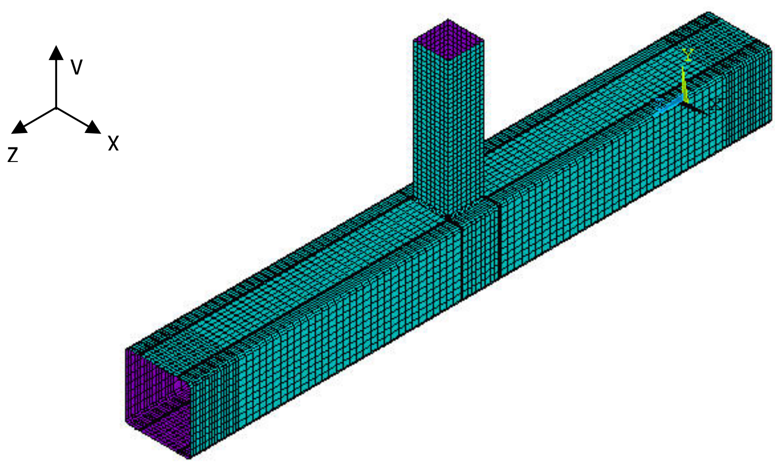

Figure 5. Numerical model for the analysis the “T” joints.

The test layout from Lie *et al.* [9] is shown in Figure 6. It was reproduced in the numerical model, not only in terms of material properties, but also in terms of the whole test geometry: span, type of support, load introduction and stiffness near the end supports. This is necessary since to establish any comparison with the results from [10], these results are in terms of load-displacement curves of the brace. In fact, this data includes deformability of the brace itself, of the chord by bending, local chord deformation near the supports, and of course deformations at the connection: chord side walls and chord loaded face deformations.

After validation of the numerical model from comparison of the above referred experimental curve, it is then possible to derive from the numerical model the most relevant contributions for the deformation, namely the behaviour of the loaded chord face.

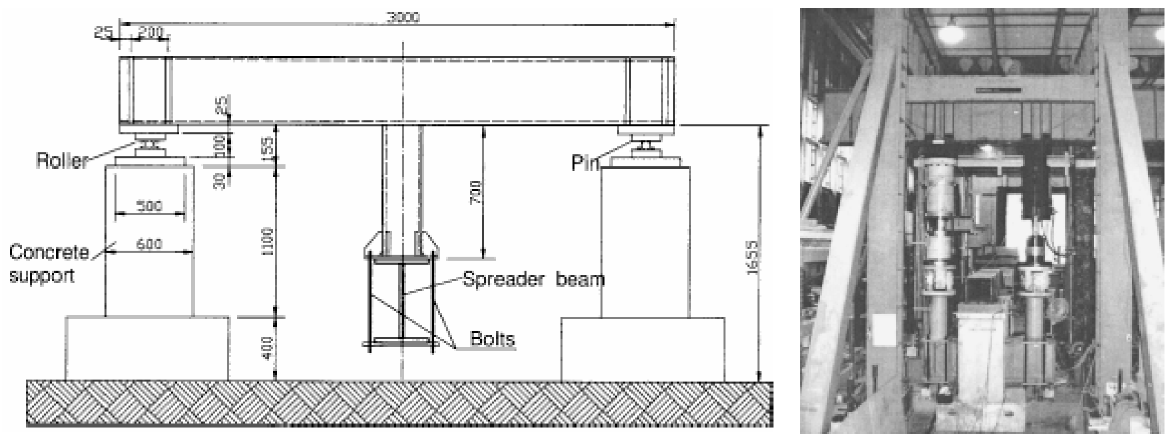

Figure 6. Experimental test layout, after Lie *et al.* [9].

For each numerical model a full material (material model was considered bilinear with 5% strain hardening) and geometric nonlinear analysis was performed. This procedure represents the full assessment of the safety of the joints, and may be summarized in several outputs, namely the stress distribution (that detects, among other data, first yielding at the connections), or the force-displacement curve for any node within the connection.

These results allow the assessment of the EN 1993-1-8 [4] performance not only in terms of maximum load (however the maximum numerical load is compared to the plastic load calculated from the Eurocode [4]), but also in terms of the whole curve. This may lead to the derivation of conclusions in terms of the stiffness and of post-limit behaviour of the chord face, namely for the assessment of the performance of deformation limits criteria for the chord face resistance, or for the evaluation of the available over-strength by membrane action.

4.2 Weld modelling

It is common practice to analyse this type of connections without any consideration of the weld, just by simply modelling the mid-surfaces of the member walls by shell elements [8], [10]. Although it is referenced by some authors that this effect may be of importance mainly in K-joints with gap, since the weld does not have a negligible size compared to the size of the gap [10], it will be shown in this paper there is some difference resulting from the fact of considering the weld effect in this T joint.

The weld was modelled firstly by using a ring of shell elements (SHELL 181 - four nodes with six d.o.f. at each node) as shown in Figure 7(a), reproducing the weld size in a similar way than proposed by Lee [10] or by van der Vegte [19] (Figure 8). In this paper the welds were modelled by solid elements (SOLID45 - eight nodes with three d.o.f. at each node) as well - Figure 7 (b) in order to properly assess its influence.

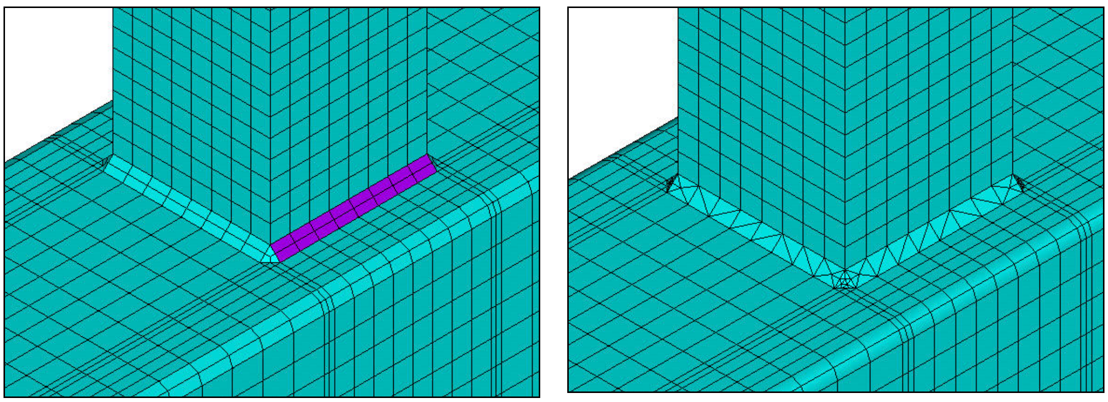

a) weld with shell elements   b) weld with solid elements

Figure 7. Numerical model for the analysis the “T” joints.

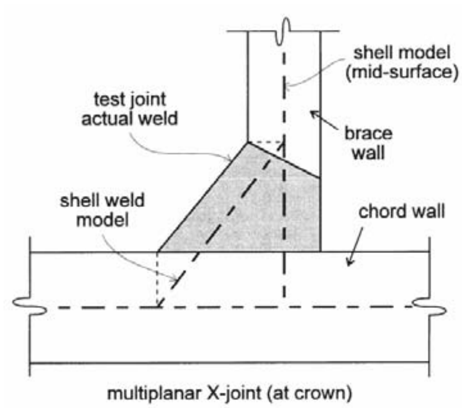

Figure 8. Modelling of the welds by shell elements after Lee [10].

4 Results Analysis

As explained before, two different models were used to consider the influence of the welds on the joint global behaviour: in the first model (T1RA4Nx2MATWELDSOLID), welds were modelled with solid elements. In the second model (T1RA4Nx2MATWELDSHELL), shell elements were used for the same purpose. A third model without weld modelling (T1RA4Nx2MATWELDOUT), was considered also in order to evidence the differences.

Figure 9(a) presents the comparison of the results from these three models, and the numerical results found in [10] for the model T1. The geometrical and mechanical properties for this model were presented in Table 1. The results comparison for the model T2 is presented in Figure 9(b). It may be observed from these curves that the model without welds is a lower limit for the joint response because the loaded effective width of the brace is smaller than when the welds are considered, and the difference is up to 13 % in the case of the model T1. It is interesting to note that, since considering the welds leads to higher values of the parameter $\beta = b_1 / b_0$, this weld modelling influence is larger for larger values of β, as results from Figure 3.

The results from modelling the welds with shells or with solids are almost the same, and therefore for the parametric study, the shell model was adopted due to computing efficiency.

As previously mentioned, when $\beta \leq 0.85$ the T joint design is governed by the plastic failure of the chord face. To verify this limit state, Figure 10 presents the von Mises stress distribution for the model T1. From this Figure it is also possible to conclude that widespread yielding corresponds approximately to a load of 523 kN, and observing Figure 9(a) this load is close to the point where the joint stiffness starts to decrease.

To evaluate the influence of the parameter β on the joint global behaviour, five models were used in a parametric analysis, keeping the same chord for all models (350x350x15). The same mechanical properties used early were adopted here as well. The braces width were 90, 180, 260 and 300 mm, that correspond to values of β of 0.25, 0.50, 0.75, 0.80 and 0.857, respectively. The results are presented in Figure 11. As expected from Figure 3, increasing the value of β leads to a strong increase in the strength of the connection specially if $\beta \leq 0{,}75$. However, if $\beta > 0{,}75$, an increase of this parameter leads to an increase of strength with a magnitude much smaller than expected from Figure 3. This is due to the fact that for large values of β bending is not leading anymore, but shear and punching shear star to dominate.

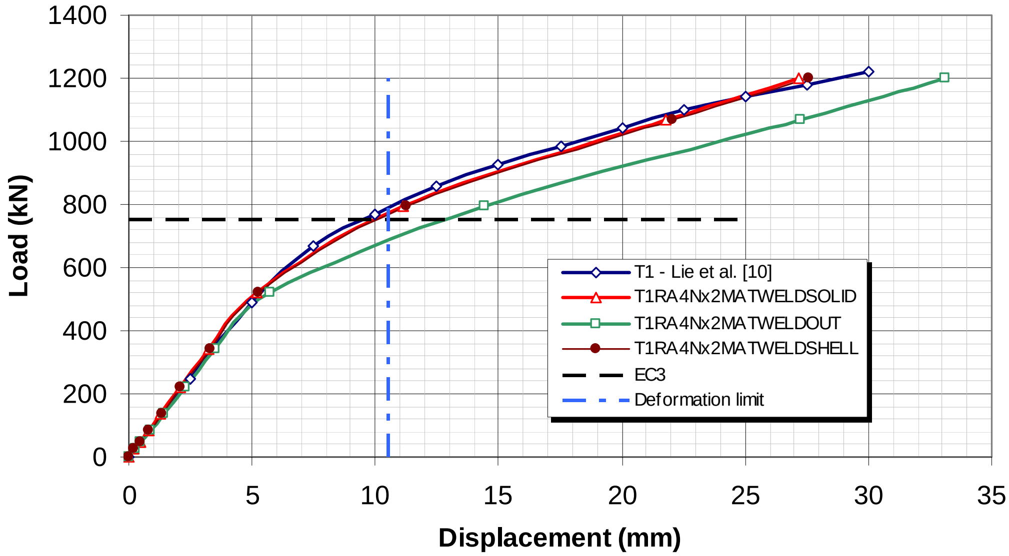

a) model T1

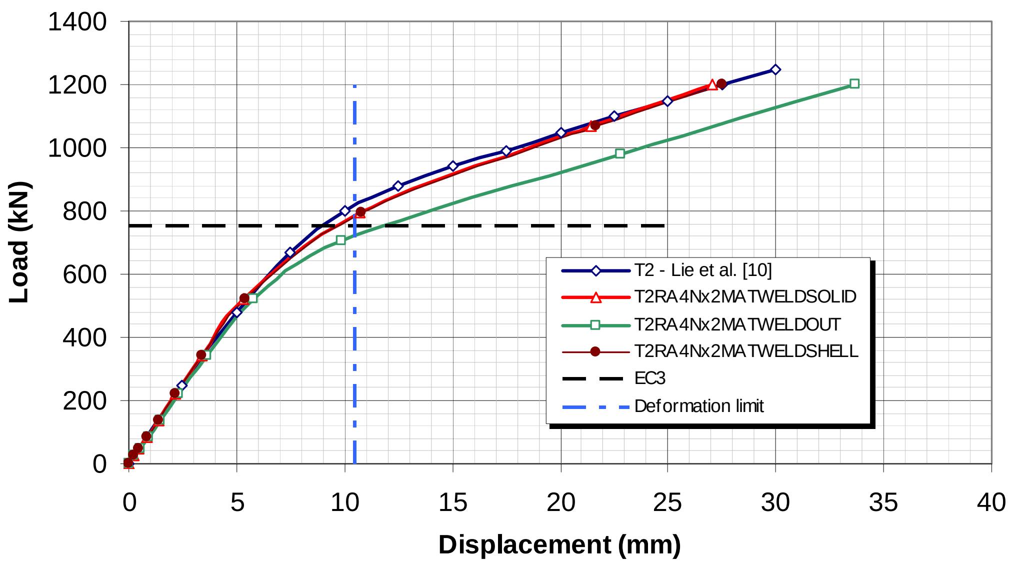

b) model T2

Figure 9. Results comparison – welds types.

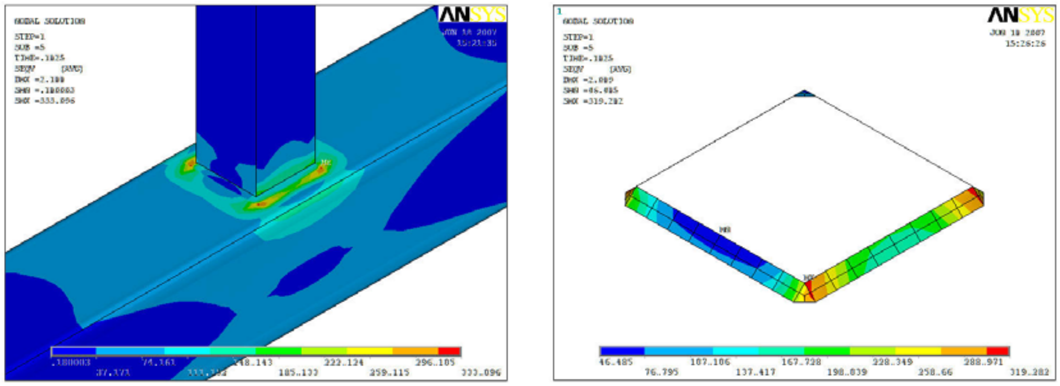

a) applied load = 219 kN

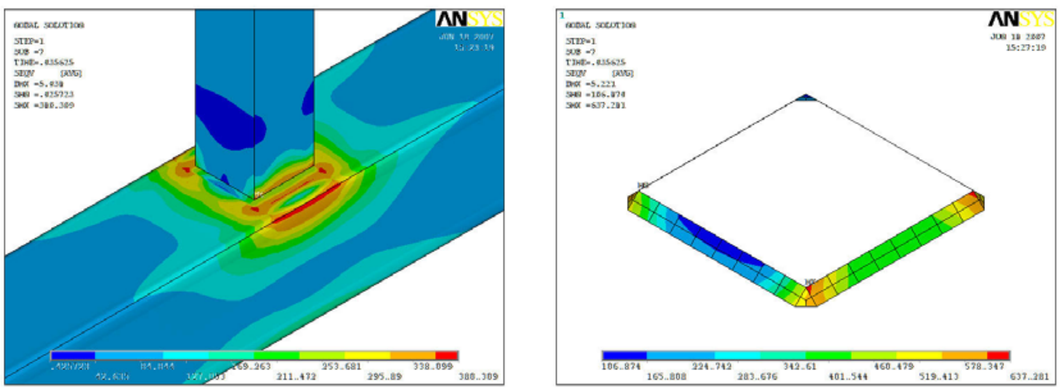

b) applied load = 523 kN

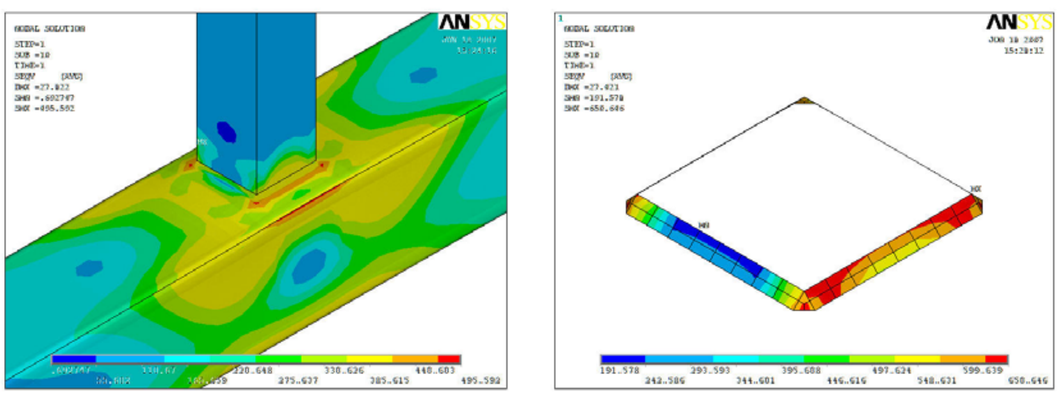

c) applied load = 1200 kN

Figure 10. Von Mises stress distribution – model T1.

The individual load *vs* displacement curves are presented in Figure 12. Through the observation of these curves, it may be concluded that the numerical results have in general a good agreement with the Eurocode 3 [4] previsions. The joint resistance was derived at a load corresponding to a limit deformation of the chord face deformation of 3% of the chord width, i.e., 10.5 mm according to the proposal of Lu *et al*. [12]. However, the last model where β = 0.857, presented different results when compared to Eurocode 3 [4] previsions. It is important to emphasize that the joint resistance for this case was evaluated by interpolation between resistances for β = 0.85 and β = 1.0, according to this code, to account for punching shear, but Eurocode results are not satisfactory. These conclusions are in line with the previous conclusions from [11].

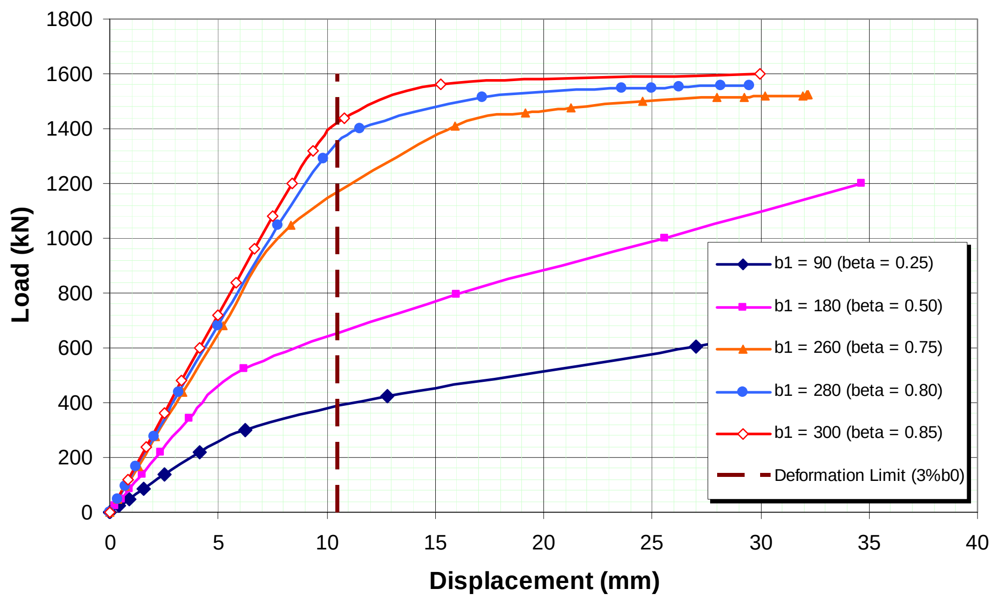

Figure 11. Load *versus* displacement curves – β variation.

5 Final Considerations

A finite element model using four-nodes thick shell elements was developed to study the behaviour of T joints. To validate the model, material and geometrical properties used in the analysis were the same used in a numerical and experimental study by Lie *et al.* [9], [10], and both results were compared.

The results of the analysis were used to assess the EN 1993-1-8 [4] performance not only in terms of maximum load, but also in terms of the whole curve.

Although it is common practice to analyse this type of connections without any consideration of the weld, it was shown in this paper there is some difference resulting from the fact of considering the weld effect in this T joint. In fact, modelling the welds led to a strength increase of up to 13 %, independently of the fact of using shell or solid elements for the welds.

A parametric analysis in terms of the parameter β was performed to evaluate the joint global behaviour, using five different joint geometries. The results show that increasing the value of β leads to a strong increase in the strength of the connection, but if $\beta > 0,75$ [18], an increase of this parameter leads to an increase of strength of a much smaller magnitude.

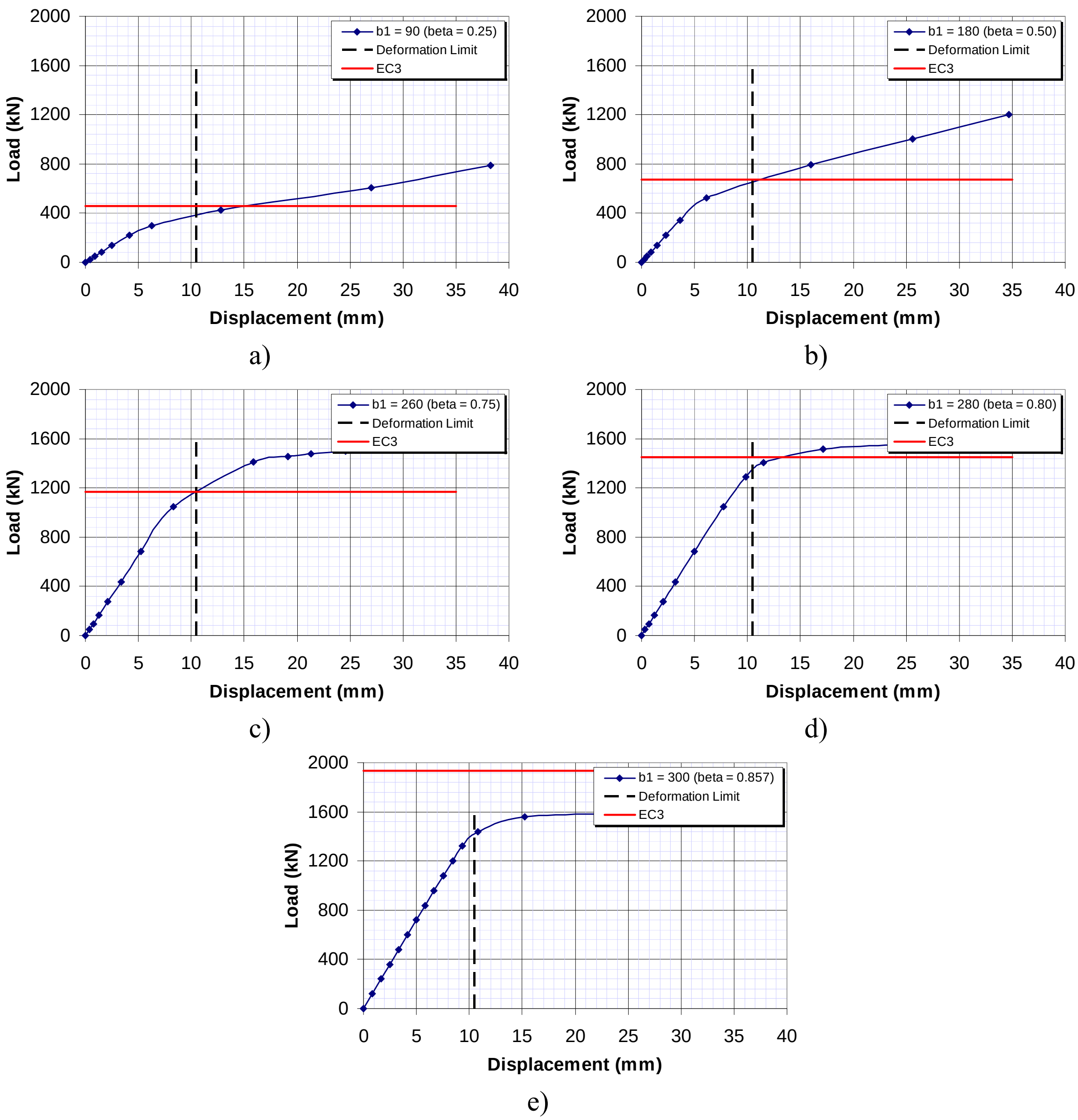

Figure 12. Load *versus* displacement individual curves.

Through the observation of the analytical curves, it may be concluded that the numerical results have in general a good agreement with the Eurocode 3 [4] previsions for the resistance combined with a 3 % deformation limit criterion for the deformation of the chord face. However, for larger values of β, Eurocode apparently does not properly account for punching shear, since unsatisfactory and unsafe results were found.

Acknowledgments

The authors thank CAPES/GRICES by the International Cooperation Program between Civil Engineering Department of the University of Coimbra, Portugal and Faculty of Engineering of the UERJ – State University of Rio de Janeiro. And also thank the CNPq and FAPERJ by the financial support to develop this research program.

References

[1] ANSYS, 1998. Swanson analysis systems, Inc., P.O. Box 65, Johnson Road, Houston, PA, 15342-0065, version 5.5, Basic analysis procedures, 2nd edition.

[2] Cao, J.J., Packer, J.A., Young, G.J., 1998. Yield line analysis of RHS connections with axial loads, *J. Constructional Steel Research,* vol. 48, nº 1, pp 1-25.

[3] Davies, G., Packer, J.A., 1982. Predicting the strenght of branch plate – RHS connections for punching shear, *Canadian Journal of Civil Engineering*, 9, nº 3, pp 458-467.

[4] Eurocode 3, EN 1993-1.8, 2005. *Design of steel structures – Part 1.8: Design of joints* ("final draft"), CEN, European Committee for Standardisation, Brussels.

[5] Gomes, F.C.T., 1990. *Etat Limite Ultime de la Résistance de L'âme d'une Colonne dans un Assemblage Semi-Rigide d'axe Faible*, Rapport Interne nº 203, MSM - Université de Liège.

[6] Korol, R., Mirza, F., 1982. Finite Element Analysis of RHS T-Joints, *Journal of the Structural Division, ASCE*, vol.108, No. ST9, pp 2081-2098.

[7] Kosteski, N., Packer, J.A., Puthli, R.S., 2003. A finite element method based yield load determination procedure for hollow structural section connections, *Journal of Constructional Steel Research,* vol. 59, nº 4, pp. 427-559.

[8] Lee, M.M.K., 1999. Strength, Stress and Fracture Analyses of Offshore Tubular Joints Using Finite Elements. *Journal of Constructional Steel Research*, vol. 51, pp. 265-286.

[9] Lie, S-T, Chiew, S-P, Lee, C-K and Yang, Z-M, 2006. Static Strength of Cracked Square Hollow Section T Joints under Axial Loads. I: Experimental. Journal of Structural Engineering, 132:3(368-377).

[10] Lie, S-T, Chiew, S-P, Lee, C-K and Yang, Z-M, 2006. Static Strength of

Cracked Square Hollow Section T Joints under Axial Loads. II: Numerical. Journal of Structural Engineering, 132:3(378-386).

[11] Lima, L. R. O. de; Neves, L. F. da C.; Silva, J. G. S. da; Vellasco, P. C. G. da S., 2005 Análise Paramétrica de Ligações T com Perfis Tubulares em Aço Através de um Modelo de Elementos Finitos. Proceedings of CILAMCE XXVI - The Iberian Latin American Congress on Computational Methods in Engineering, p. 1-12 (CD-ROM).

[12] Lu, L.H., de Winkel, G.D., Yu, Y., Wardenier, J., 1994. Deformation limit for the ultimate strength of hollow section joints, *6th International Symposium on Tubular Structures*, Melbourne, Australia, pp 341-347.

[13] Neves, L.F. C., Lima, L. R. O. de, Jordão, S. and Silva, J. G. S. da, 2005. Structural Analysis of “T” and “KT” Joints of a Steel Truss Structure Using the Finite Element Method. *Proceedings of the Tenth International Conference on Civil, Structural and Environmental Engineering Computing,* Civil-Comp Press, Stirling, Scotland, pp. 1-15.

[14] Neves, L.F.C., 2004. *Monotonic and Cyclic Behaviour of Minor-axis and Hollow Section Joints in Steel and Composite Structures*, Doctoral Thesis, University of Coimbra, 2004.

[15] Packer, J. A., Wardenier, J., Kurobane, Y., Dutta, D. and Yoemans, N., 1992. Design Guide for Rectangular Hollow Section (RHS) Joints Under Predominantly Static Loading, CIDECT - Construction with Hollow Steel Sections, Verlag TÜV Rheinland.

[16] Packer, J.A. Morris, G., Davies, G., A Limit States Design Method for welded Tension Connections to I Section Webs, *J. Constructional Steel Research, vol. 12 (1989)*, pp. 33-53.

[17] Packer, J.A., 1993. Moment Connections between Rectangular Hollow Sections, *J.Constructional Steel Research 25*, pp 63-81.

[18] TABET, Felipe, LIMA, Luciano Rodrigues Ornelas de, VELLASCO, Pedro Colmar Gonçalves da Silva, ANDRADE, Sebastião Arthur Lopes de, SILVA, José Guilherme Santos da, NEVES, Luis Filipe da Costa, Avaliação do coeficiente de eficiência em ligações “T” com perfis tubulares através do método dos elementos finitos, *Proceedings of the XXVII CILAMCE – Iberian Latin American Congress on Computational Methods in Engineering*, September 3-6, Belém-PA, Brasil, pp 1-14.

[19] Van der Vegte GT, de Koning CHM, Puthli RS, Wardenier J., Numerical simulation of experiements on multiplanar steel X-joints. International Journal of Offshore and Polar Engineering 1991, 1(3), pp 200-2007.

[20] Zhao, X, Hancock, G., 1991. T-Joints in Rectangular Hollow Sections Subject to Combined Actions, *Journal of the Structural Division, ASCE, vol.117, No. 8*, pp2258-2277.